# Competing intermediates in the pressure-induced wurtzite to rocksalt phase transition in ZnO

Salah Eddine Boulfelfel and Stefano Leoni[*]

*Max-Planck-Institut für Chemische Physik fester Stoffe, 01187 Dresden, Germany*

Molecular-dynamics simulations are carried out on the wurtzitelike ($B4$) to rocksaltlike structure ($B1$) pressure-induced phase transition in ZnO. A tetragonal intermediate ($iT$) appears at the $B4/B1$ interface along the transition. A hexagonal intermediate ($iH$) of $h$-BN type is also occasionally visited, as a result of axial compression, which however does not represent a necessary step for the transition. The presence of small fractions of rocksalt or defects after $B1 \rightarrow B4$ back transformation is traced back to the competition between deformation modes connected to $iT$ or $iH$.

## I. INTRODUCTION

Metal oxides occupy a privileged place in modern materials science due to a broad range of interesting properties. Their advantageous electronic properties open new perspectives in electronic and optoelectronic industry.[1] In this view, zinc oxide or zincite, $n$-type semiconductor with a direct band gap of 3.2 eV, is a good laser and UV light emitter besides numerous other technological applications (e.g., chemical sensor, catalyst, piezoelectric transducer, and solar cells).[2]

The polymorphism of ZnO encompasses three structure types. The ambient conditions wurtzitelike structure $B4$, the zinc-blende metastable variety $B3$, and the high-pressure modification, which adopts the rocksaltlike structure $B1$. The wide indirect band gap (2.45 eV) of the cubic phase $B1$ makes it more suitable for high $p$-type doping than the hexagonal variant.[3] Trapping the rocksalt structure at ambient conditions is therefore of great interest.

The first indication of a first-order pressure-induced phase transition to the rocksaltlike structure ($B1$), at ~10 GPa, was reported by Bates *et al.*[4] The $B4$-$B1$ transition has been characterized to be fully reversible with a pronounced hysteresis (2–10 GPa).[5–7] However, other reports have found that a large fraction of the rocksaltlike $B1$ phase persists during decompression and can be partially quenched at ambient conditions.[3,8,9] Nonetheless, the manipulation of the nanoscale grain size plays a major role in the delay of the $B1$-$B4$ phase transition and could be the key to fully quench the $B1$ phase of ZnO.[4,10] Along this line, several experimental studies have been undertaken to explore the high-pressure stability of ZnO polymorphs,[11–15] as well as the transformation thereof associated, leading to various transition models.[16–19]

Orientation relations between unit cells of the wurtzitelike and the rocksaltlike phases collected during high-pressure x-ray investigation on ZnO single crystals have been used to derive transformation mechanisms.[18] Combined with symmetry considerations, the deformation between $B4$ ($P6_3mc$) and $B1$ ($Fm\bar{3}m$) is described as a continuous transformation through a common orthorhombic subgroup $Cmc2_1$. Based on this model, first-principles investigations suggested a similar homogenous orthorhombic deformation path going through a fivefold hexagonal intermediate structure ($iH$) isostructural to $h$ BN.[20] This model implies a variation of the internal structural parameter $u$ ($u$ is a relative lattice spacing between the Zn and O sublattice) during the first step $B4 \rightarrow iH$. Rietveld refinement study of the pressure dependence of $u$ in the wurtzite supports the orthorhombic deformation path $B4$-$iH$-$B1$.[9]

Phase transitions induced by temperature or pressure are often associated with different optic and elastic instabilities. Although the first-order pressure-induced $B4$-$B1$ transition cannot be carried by a single mode, becoming soft across the transition, shear modes and phonon modes softening appear as precursors to structural transformation in ZnO.[12,17,19] The ZnO wurtzite phase shows $\Gamma$ point optic modes of $A_1 + 2B_2 + E_1 + 2E_2$ symmetry character ($A_1$, $E_1$, and $E_2$ are Raman active while $A_1$ and $E_1$ are infrared active).[19] The transition model $B4$-$iH$-$B1$ suggests the optic $A_1$ and $E_2^{high}$ modes to be affected by the first step $B4$-$iH$.[21] However, high-pressure Raman spectroscopy investigations show no instability of these modes during the transition.[19] The only Grüneisen parameter that shows a negative value corresponds to $E_2^{low}$ mode. In fact, this instability, together with the softening of shear modes under pressure, may involve another type of wurtzite distortion.[12] In a common monoclinic orientation, atomic displacements can be continuously mapped through a fivefold tetragonal intermediate structure ($iT$).[22] However, up to date, neither intermediate ($iH$ and $iT$) has been characterized in experiments.

The two transition route models ($B4$-$iH$-$B1$ and $B4$-$iT$-$B1$) find support in certain aspects of the experimental evidence, revealing only parts of a possibly more articulated picture. In combination with *ab initio* calculations typically based on adiabatic approximations, model mechanisms are weighted on an exclusivity principle in search of the better scoring one. Such an approach may considerably narrow their efficiency and may even reinforce discrepancies instead of achieving mutual completion. This challenge raised by the yet unresolved question of the transformation mechanism in ZnO, despite recent experimental and theoretical efforts, has prompted our interest in a detailed mechanistic investigation, in the attempt to reconcile different experimental observations.

In this work, to elucidate the mechanism of the pressure-induced phase transition in ZnO, we identify different stages of the transformation and we provide a complete atomistic
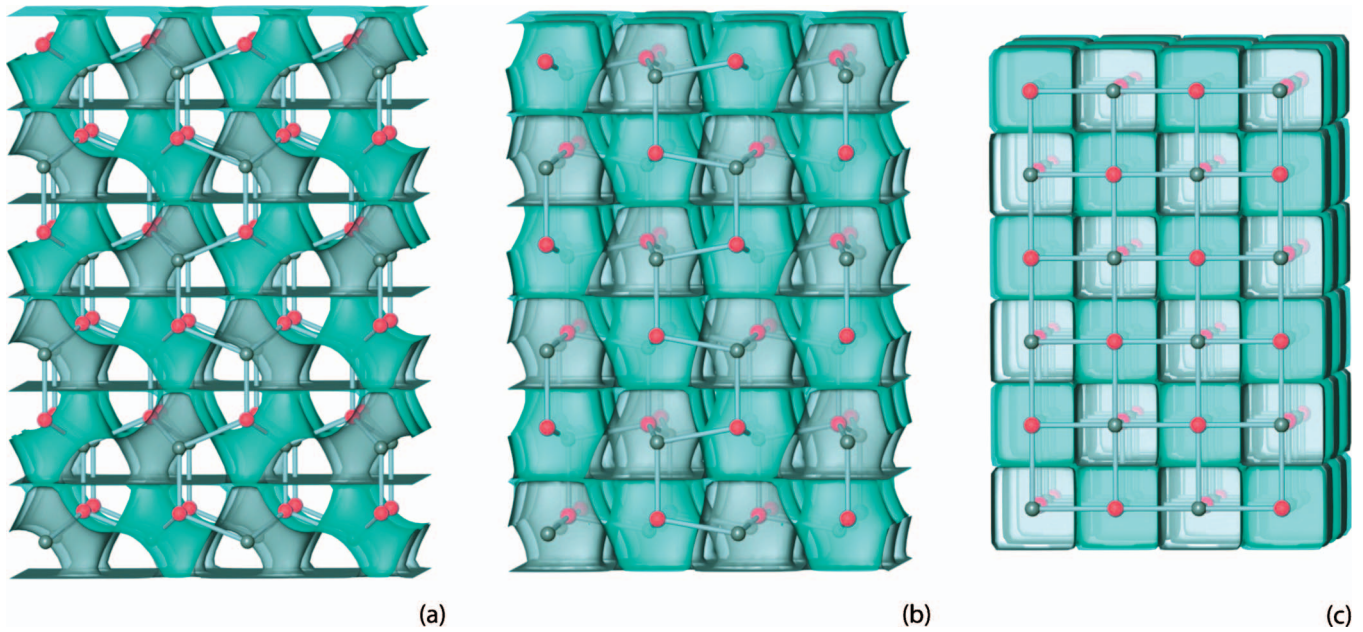
FIG. 1. (Color) Model transformation mapping the network of (a) *B*4 onto the network of (c) *B*1. The Zn (gray) and O (red) atom sets are separated from each other by a PNS (the corresponding gray/green manifold is displayed). The latter develops perpendicularly with respect to shortest Zn-O connections. Figure 1(b) represents an intermediate between (a) and (c). More details are given in the text

description of hexagonal *B*4 phase reconstruction into cubic *B*1. The relevance of the proposed intermediate structures (hexagonal *iH* and tetragonal *iT*) and their appearance as structural motifs along the transformation are discussed with reference to experimental evidences.

To achieve a reliable and detailed mechanistic picture, we employ a simulation strategy that combines isothermic-isobaric (NpT) molecular dynamics with transition path sampling (TPS).[23] This methodology has proven very effective in the simulation of activated processes[24] with phase coexistence and phase growth.[25–28]

## II. SIMULATION DETAILS

TPS is a generalization of Monte Carlo (MC) procedures in the space of trajectories connecting two states (*B*4 and *B*1 in this case) separated by a high barrier in a rough energy landscape.[23] Therein the relevance of a transition route is biased to path probability. The overall simulation approach is iterative and develops from an initial trajectory.[23,24]

In analogy with conventional MC simulations, the first phase of TPS consists of equilibrating an initial pathway in order to gradually shift the trajectory regime to more probable regions. Accordingly, the first trajectory (FT) does not need to be a probable one.

However, the intelligent design of the first trajectory affects the calculation performance in terms of the number of TPS moves required to achieve trajectory decorrelation from the initial regime. On the other hand, different starting points may give access to different intermediate regimes *along* the decorrelation process. Therefore, for the *B*4-*B*1 transformation, we used a geometric-topological approach based on transforming periodic nodal surfaces.[29–34] This method provides a means to extract intermediate configurations between

*B*4-*B*1 along distinct *quasi*orthogonal paths (with respect to the deformation modes coded therein), with a (typically concerted) nonlinear mapping of atomic positions from the initial (*B*4) to the final (*B*1) configurations. This approach has many immediate advantages. (i) Initial very high-energy/high-strain configurations can be avoided. (ii) Independent TPS runs can be started from distinct initial mechanistic regimes. (iii) Different features can be coded in the initial path. Additionally, many initial mechanisms can be checked for their convergence toward the same final mechanistic regime after TPS processing.

Our modeling approach is illustrated in Fig. 1. Figures 1(a) and 1(c) show the *B*4 and *B*1 networks with a periodic nodal surface (PNS) wrapped around each one of them. Such a surface is calculated from a short Fourier summation, like it is described in Refs. 30–34, and is chosen such that the zeroth value isosurface develops perpendicular to the Zn-O shortest connections [Figs. 1(a)–1(c)]. Like this, the Zn atoms are placed on the positive side (blue side) of the surface, while the O atoms on the negative one (gray side). This offers a means to code the whole atomic arrangement into a single parametric expression. From the limiting functions [Figs. 1(a) and 1(c)], a dense set of intermediates can then be derived by interpolation.[33] The configuration and the surface corresponding to the middle point are given in Fig. 1(b). The shown deformation corresponds to vertically shortening a set of Zn-O connections.

In this work, the mechanistic elucidation of the *B*4-*B*1 transformation in ZnO develops along the investigation of the relevance of intermediate configurations, referred to as *iT* or *iH*. It is therefore crucial to have a means to generate initial regimes, which are able to visit different intermediates. This is achieved in the modeling approach. While we bypass on purpose the intermediates in the topological mod-

eling step, we find that different initial trajectories favor the appearance of one or the other intermediate. Along this line, a precise investigation of trajectory evolution, which is able to capture the relevance of intermediate configurations, can be tackled.[35]

The average coordination number of the cations is used as an order parameter to distinguish between $B1$ (CN=6) and $B4$ (CN=4). Clearly, apart from enabling a quick detection of emerging intermediate pattern (CN=5 for both $iH$ and $iT$), this does not enforce a particular evolution of the coordination number during TPS. While the CN typically increases as an effect of pressure, no bias is imposed on it.

Within the NpT ensemble, momentum modifications are applied to snapshots taken from the initial trajectory while keeping total energy, momentum, and angular momentum unchanged.[24] The momentum modifications are random and Gauss distributed, in order to keep a good balance between trajectory modification and acceptance rate. The propagation of the new configuration in both directions of time provides a new trajectory that is examined for the $B4$-$B1$ transformation. The initial trajectory is replaced by the new successful one and the procedure is iterated. For each TPS move, the momentum modification probability is required to be smaller than a random number selected from a uniform distribution. Otherwise, the modification is rejected and the move is repeated. A total of three inital trajectories were used, representing as many distinct geometric mechanisms.

The simulation box contained 768 Zn-O pairs. For the interatomic interactions, a set of empirical force field parameters[36] was used. Many parameters have been proposed for ZnO (Refs. [37–40]) with different scopes. The parametrization of Binks and Grimes,[36] derived from Lewis and Catlow,[39] guarantees a reliable reproduction of transition pressure, structural parameters, elastic constants, and dielectric constants[41] of the ZnO polymorphs compared to experiments and *ab initio* calculations.[42] To further validate the energetics of the force field, we performed density-functional theory (DFT) calculations.[43] The energy sequence obtained from DFT generalized gradient approximation (Perdew-Burke-Ernzerhof parametrization of the exchange-correlation functional[44]) total-energy calculations is correctly reproduced by the force field: $B4 < B1 < iH \leq iT$.

To explore the effect of pressure on the mechanism of transformation and the stability of possible intermediates involved therein, we performed different sets of simulations at different pressures ranging from 9 to 15 GPa. The temperature was kept equal to the experimental value of 300 K.

The molecular-dynamics simulations were carried out using the DLPOLY package.[45] A relatively small simulation time step of 0.2 fs was used in order to ensure a good time reversibility. The Melchionna/Nose-Hoover algorithm[46] ensured constant pressure and temperature. Therein, anisotropic shape changes of the simulation box were allowed.

### III. RESULTS

The set of transition pathways harvested in the course of TPS iterations shows a quick departure of the trajectory regime from the collective motion inherited from the geometric modeling, like the one displayed in Fig. 1. Within 10–15 iterations, the initial trajectories crossing well-ordered atomic configurations are lifted in favor of a different typically noncollective mechanism characterized by coexisting structural motifs [Fig. 2]. The first indication of decorrelation in the trajectory regime is the setup of a layer shearing mechanism. Within $(001)_{B4}$ layers, adjacent hexagons are deformed into squares. Locally, hexagons can be compressed either along [120] or [210]. On a larger scale, the combination of these two fashions pins $(001)_{B4}$ layer shearing direction along [110]. The high-pressure phase $B1$ sets in as a slab. Further growth is achieved perpendicularly to the direction of the shearing. Therein, an intermediate tetragonal structure $iT$ (space group $I4mm$) appears at the interface between $B1$ phase and the transforming $B4$ phase (Fig. 3 left). The overall reconstruction of $(001)_{B4}$ layers consists of a combination of parallel and antiparallel layer displacements along [110] in a zigzag fashion [Fig. 1(a)]. Such combination avoids excessive strain during the phase transition with respect to a mechanism where all hexagons are compressed along a unique direction {either [210] or [120]}. Consequently, the [100] direction in the rocksaltlike structure is no longer parallel to [100] in the wurtzite. This change in morphology during the transition finds support in the recent experimental observations of crystallographic direction relations between the initial and final crystallites.[18] The angle spanned by the two directions ($[100]_{B4}$ and $[100]_{B1}$) after transformation was found to be ~15° in both experiments and in our simulations.

While the change in sample orientation is in accordance with the transformation mechanism described above, a study of pressure dependence of the internal structural parameter $u$ in the wurtzite phase of ZnO is pleading in favor of another transition model.[9] Using high-resolution angular dispersive x-ray diffraction up to 12 GPa, the structural parameter $u$ is found to increase with pressure. This would be consistent with the orthorhombic distortion path where $u$ initially varies from 0.38 to 0.5 leading to a hexagonal intermediate structure $iH$ of space group $P6_3/mmc$.

This apparent discrepancy can be resolved considering the complete set of reactive pathways collected in the course of simulations. Therein the relevance of a mechanism is related to the probability of finding corresponding dynamical pathways.[24]

In the course of TPS, transition trajectories cross different regimes before the more probable favorite one sets in. Mechanisms corresponding to the decorrelated trajectory regime share the same (001) overall layer shearing features (Fig. 2). However, different intermediate structures may occur during transformation, depending on the peculiar evolution of independent TPS, which started from distinct FT. We recall that both intermediate structures ($iH$ and $iT$) were bypassed on purpose during the generation of the FT and that their appearance reflects system preferences, not an external bias. Therefore, from the collected trajectories, we can learn about the reason of their spontaneous emergence. Either $iH$ or $iT$ is formed by a different synchronization of the variation of relative spacing $u$ between cations and anions sublattices with $(001)_{B4}$ layers shearing. If the compression along $[001]_{B4}$ occurs during (or after) the $(001)_{B4}$ layers recon-
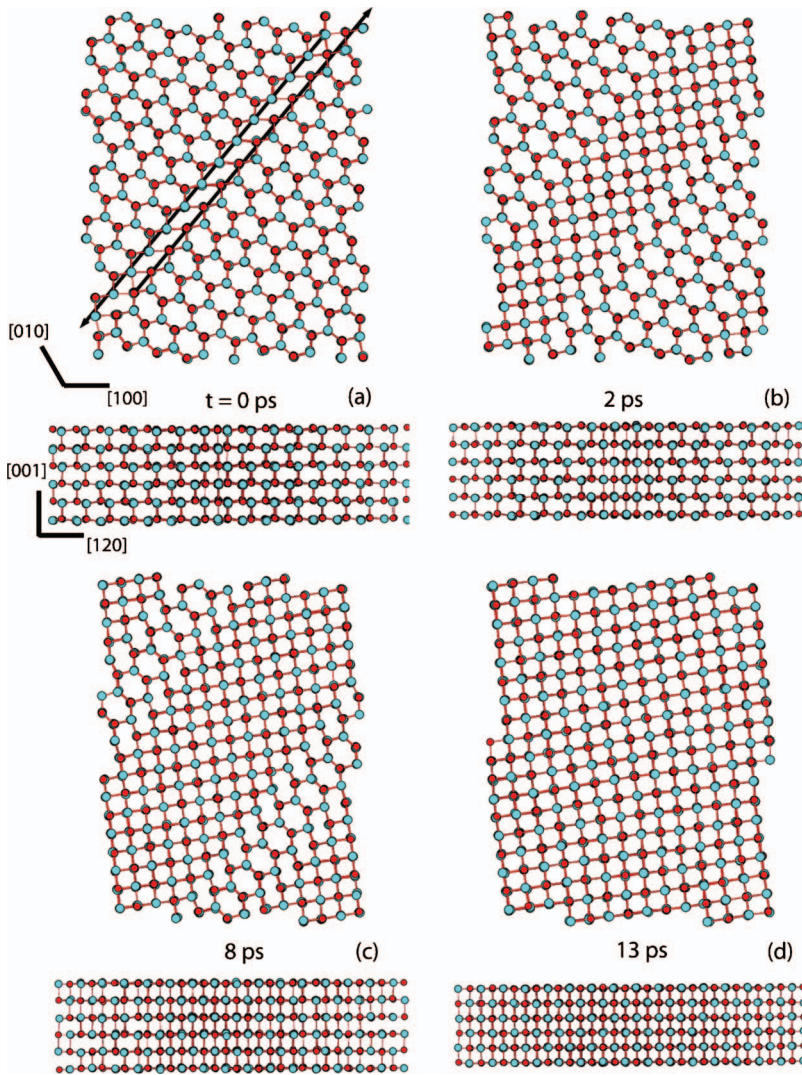
FIG. 2. (Color) Mechanism of the $B4$-$B1$ network reconstruction. The mechanism is characterized by layer shearing and by structural motif coexistence. An interface of $iT$ structural pattern appears between the forming $B1$ and the transforming $B4$, (b), and (c). (a) The antiparallel layer displacements are indicated with black arrows.

struction, the hexagonal intermediate $iH$ is ruled out and the system crosses over directly to the tetragonal $iT$ intermediate; otherwise, a compression along $c$ prior to the shearing leads to the hexagonal intermediate.

A representative intermediate regime, which is visited during TPS, is shown in Fig. 4. Therein, on the eve of $(001)_{B4}$ layers reconstruction, a change in the structure occurs [Figs. 4(a) and 4(b)]. The $B4$ phase is compressed
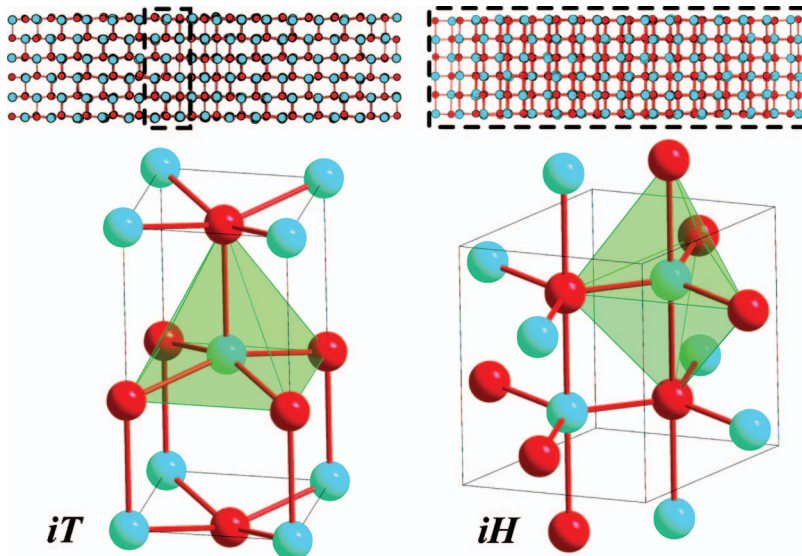


FIG. 3. (Color) Intermediate motifs $iT$ (left) and $iH$ (upper part) appearing during distinct TPS simulation runs. The former is characteristic of the interface between $B4$ and $B1$, along the displacing layers. The latter results from a more collective displacement mode. Local configurations of $iT$ and $iH$ are detailed at the bottom of figure.
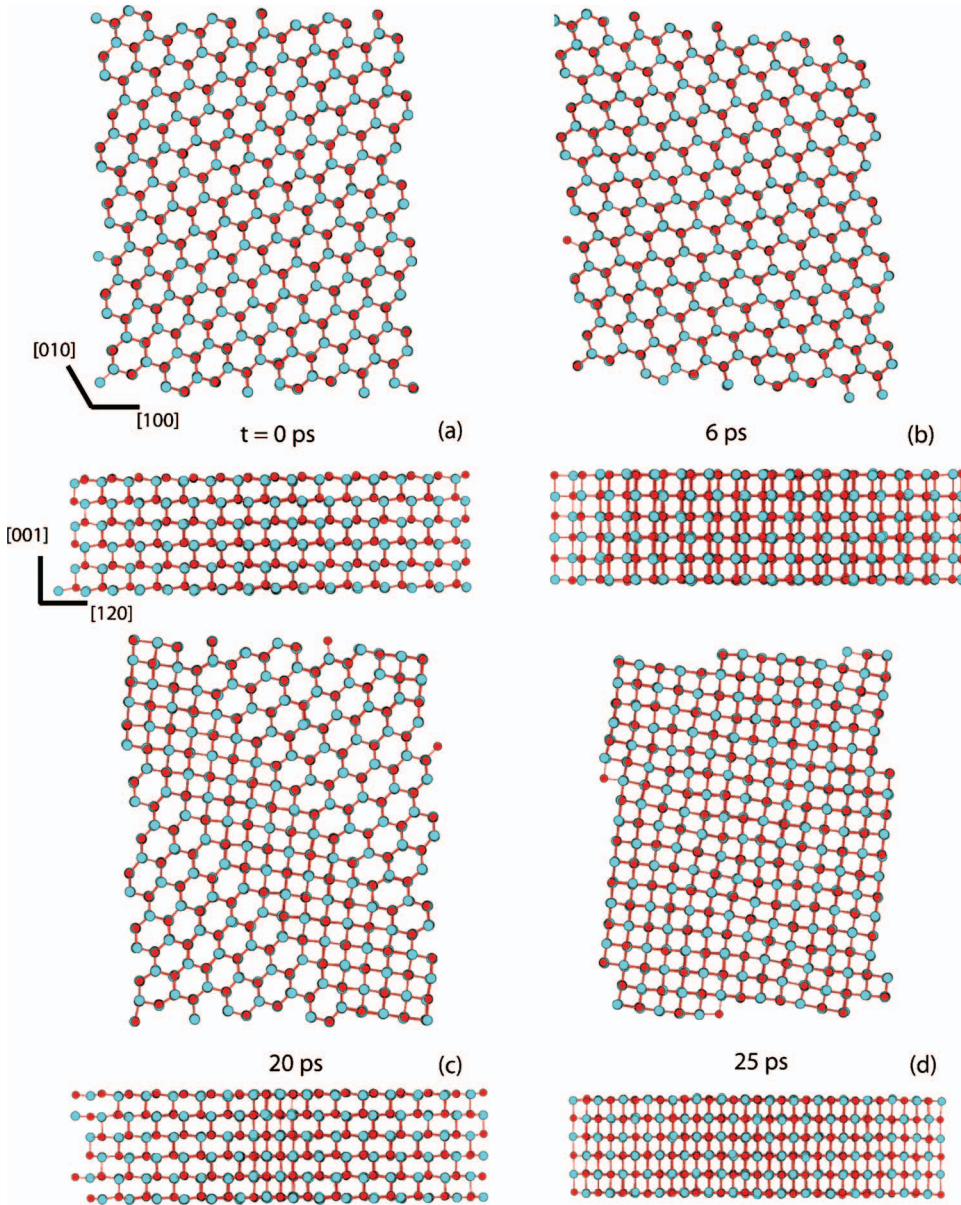
FIG. 4. (Color) (b) Transformation path crossing the $iH$ intermediate. (c) and (d) A configuration corresponding to the hexagonal intermediate $iH$ is initially visited, before the transformation to $B1$ resumes via layer shearing.

along $c$ such that new contacts appear all along. The atoms are *quasi*collectively displaced parallel to $[001]_{B4}$ and the whole system is converted into a hexagonal fivefold intermediate structure $iH$ [Fig. 3 right and Fig. 4(b)]. The internal parameter $u$ changes from 0.38 to 0.5. However, as soon as the reconstruction of $(001)_{B4}$ layers resumes, atoms regain their initial positions within the wurtzite structure under the reversal of the $B4 \rightarrow iH$ transformation. The value of $u$ is again 0.38 when the rocksalt phase starts forming. With respect to the layer shearing modes, which are productive toward lattice reconstruction into $B1$, the details of the transition are the same as shown in Fig. 2 and as described above. This discloses a scenario of fluctuation of $u$ close to the phase transition.

Indeed, Liu *et al.*[9] showed that the increase in the structural internal parameter $u$ is observed up to $\sim 9$ GPa with a maximal value $u = 0.43$ at around 5.6 GPa, well below the critical pressure of 10 GPa and before the appearance of the $B1$ phase. As the rocksalt structure starts forming, the param-

eter $u$ shows a sharp decrease to its initial value of 0.38. This reversible pretransitional effect reported in experiments is reproduced in our simulations (Fig. 4).

The $B4$-$B1$ transition in ZnO is accompanied by a large volume collapse ($\sim 20\%$).[12] Considering the profile of the volume evolution associated with paths containing the $B4$-$iH$ pretransitional step (Fig. 5, continuous line) or directly crossing over to $B1$ over the $iT$ intermediate (Fig. 5, dashed line), the former allows for a slightly higher maximum. The associated [001] compression implies a comparatively smaller orthogonal expansion. The cell and volume evolution anisotropy, which is difficult to trace in experiments,[16] can nonetheless be investigated in the simulations. The occurrence of the $iH$ structural pattern results into longer transition paths (25 ps instead of 13 ps). Increasing pressure above 10 GPa shortens the trajectories and alters completely the pretransitional step $B4$-$iH$ in favor of $B4$-$iT$-$B1$ path, with an overall volume variation similar to the dashed curve of Fig. 5. This supports an interpretation of the $iH$ intermediate as con-
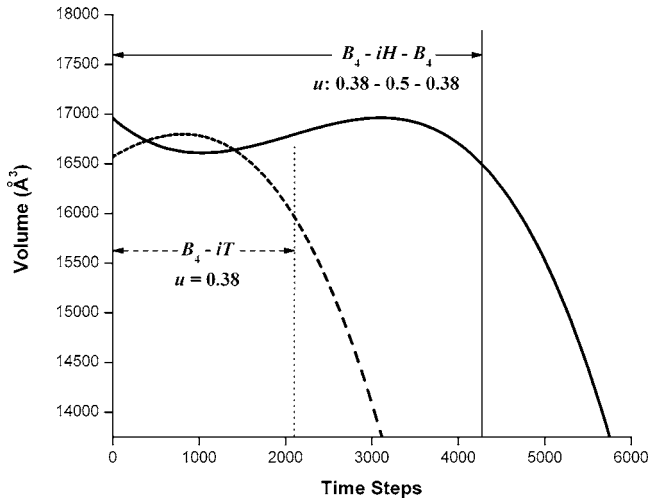
FIG. 5. Volume profiles of transitions paths visiting the $iH$ (continuous line) or bypassing it (dashed line). A different evolution of the internal parameter $u$ distinguishes the two paths, as well as a larger volume increase for the black path. The latter is disfavored by a pressure increase, and, in general, does not represent a necessary step for the transition. Details are in the text.

trolled by a fluctuation of the $u$ parameter close to phase transition and corresponding to different responses of the system to external pressure loadings.

The simulation can access regions of intermediate pressures, where concurring deformation modes can be initiated. Clearly, only one mechanism is productive with respect to transforming the system from $B4$ to $B1$. Nonetheless, the intermediate regime is far more complex, due to structural motifs and deformation modes coexistence, which accounts for the richness and apparent contradiction of the experimental data. The difference in the elastic response along $c$ and perpendicular to it—peculiar to ZnO—can be used to predict novel structural patterns, for example, in ZnO nanorods, if an external tensile load is applied.[47]

The shift in trajectories regime from the less favored ($B4$-$iH$-$B1$) to the final mechanism ($B4$-$iT$-$B1$) is thus marked by a competition between characteristic intermediate structures, hexagonal $iH$, and tetragonal $iT$. Accordingly, the response of different regions in the system may lead to irregular arrangements. On the reverse transition $B1 \rightarrow B4$, the growth of the wurtzite phase is ensured by $(001)_{B1}$ layers reconstruction into $(001)_{B4}$ layers [Figs. 6(a) and 6(b)]. The interplay between deformation modes causes the survival of a small island of cubic rocksalt phase [Fig. 6(c)], which evolves into an interface parallel to $[100]_{B4}$ [Fig. 6(e)]. Therein, rocksalt structure is formed by, in turn, deforming hexagons along $[210]_{B4}$. Interface formation along $[100]_{B4}$ induces 4- and 8-membered ring and defects, persisting in the wurtzite structure after structural relaxation [Fig. 6(f)].

Similar defects are common in wurtzite growth experiments where domains settle into low-energy configurations with grain-boundary dislocations.[48]

## IV. CONCLUSION

In conclusion, we performed molecular-dynamics simulations on the pressure-induced phase transition of zinc oxide. The transition from the hexagonal wurtzite ($B4$) to the cubic rocksalt ($B1$) structures is achieved via layer shearing over a tetragonal intermediate structure appearing at the interface between $B4$ and $B1$. In the intermediate region of the transition, a hexagonal intermediate $iH$ may appear before the reconstructive step as a result of stress fluctuations reflected in changes of the parameter $u$. The latter is in very good agree-
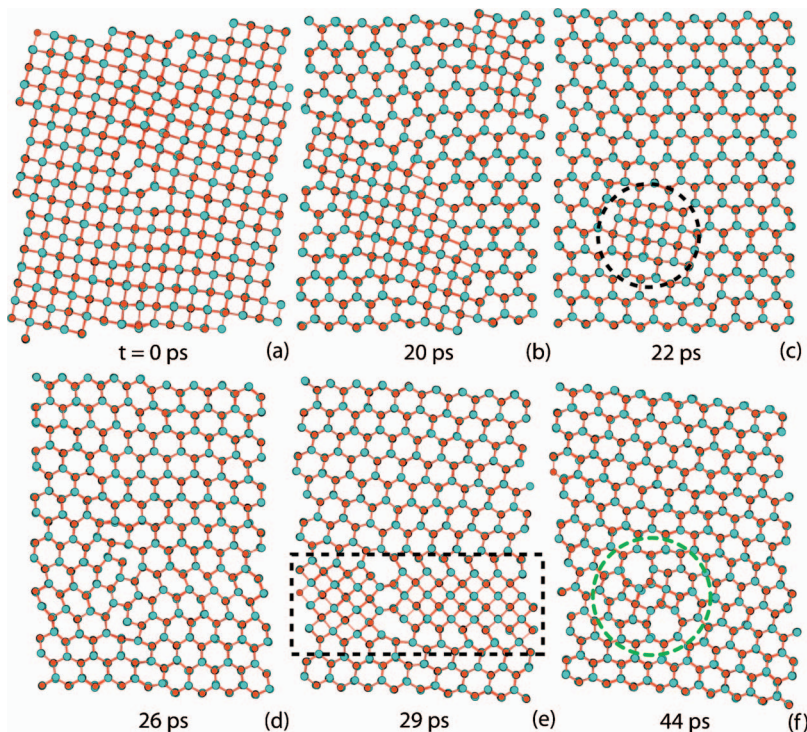


FIG. 6. (Color) (c) Permanence of $B1$ islands within $B4$ during back transformation from $B1$ to $B4$. The concurrence between deformation modes leading to different intermediates is responsible for the trapping of $B1$ motifs, as well as for defect formation. (f) The latter are characterized by eight and four rings.

ment with an experimental evidence of its evolution under pressure. The details of the mechanism are in accordance with experimental observations on sample orientation as well as spectroscopy evidence of shear and phonon modes softening under pressure. Within a scenario of competing deformation modes close to phase transition, the possible occurrence of different intermediates is explained, reconciling many experimental observations. The coexistence of deformation modes connected with both $iT$ and $iH$ intermediates may trap $B1$ islands within $B4$ during $B1$-$B4$ back transformation and

is responsible for the formation of structural defects within $B4$. An articulated yet consistent mechanistic elucidation is the overall result of our approach.

*leoni@cpfs.mpg.de.

[1] J. L. G. Fierro, *Metal Oxides: Chemistry and Applications*, 1st ed (Taylor & Francis, London/LLC, 195, 2005).

[2] Ü. Özgür, Ya. I. Alivov, C. Liu, A. Teke, M. A. Reshchikov, S. Doğan, V. Avrutin, S.-J. Cho, and H. Morkoç, J. Appl. Phys. **98**, 041301 (2005).

[3] F. Decremps, J. Pellicer-Porres, F. Datchi, J. P. Itié, A. Polian, F. Baudelet, and J. Z. Jiang, Appl. Phys. Lett. **81**, 4820 (2002).

[4] C. H. Bates, W. B. White, and R. Roy, Science **137**, 993 (1962).

[5] F. Decremps, J. Zhang, and R. C. Liebermann, Europhys. Lett. **51**, 268 (2000).

[6] H. Karzel, W. Potzel, M. Kofferlein, W. Schiessl, M. Steiner, U. Hiller, G. M. Kalvius, D. W. Mitchell, T. P. Das, P. Blaha, K. Schwarz, and M. P. Pasternak, Phys. Rev. B **53**, 11425 (1996).

[7] S. Desgreniers, Phys. Rev. B **58**, 14102 (1998).

[8] L. Gerward and J. S. Olsen, Synchrotron Radiat. **2**, 233 (1995).

[9] H. Liu, Y. Ding, M. Somayazulu, J. Qian, J. Shu, D. Häusermann, and H. K. Mao, Phys. Rev. B **71**, 212103 (2005).

[10] J. Z. Jiang, J. S. Olsen, L. Gerward, D. Frost, D. Rubie, and J. Peyronneau, Europhys. Lett. **50**, 48 (2000).

[11] J. M. Recio, M. A. Blanco, V. Luaña, R. Pandey, L. Gerward, and J. S. Olsen Phys. Rev. B **58**, 8949 (1998).

[12] F. Decremps, J. Zhang, B. Li, and R. C. Liebermann, Phys. Rev. B **63**, 224105 (2001).

[13] F. J. Manjón, K. Syassen, and R. Lauck, High Press. Res. **22**, 299 (2002).

[14] Y. Mori, N. Niiya, K. Ukegawa, T. Mizuno, K. Takarabe, and A. L. Ruoff, Phys. Status Solidi B **241**, 3198 (2004).

[15] H. Liu, J. S. Tse, and H. Mao, J. Appl. Phys. **100**, 093509 (2006).

[16] F. Decremps, F. Datchi, A. M. Saitta, A. Polian, S. Pascarelli, A. Di Cicco, J. P. Itié, and F. Baudelet, Phys. Rev. B **68**, 104101 (2003).

[17] A. Mujica, A. Rubio, A. Muñoz, and R. J. Needs, Rev. Mod. Phys. **75**, 863 (2003).

[18] H. Sowa, and H. Ahsbahs, J. Appl. Crystallogr. **39**, 169 (2006).

[19] F. Decremps, J. Pellicer-Porres, A. M. Saitta, J. C. Chervin, and A. Polian, Phys. Rev. B **65**, 092101 (2002).

[20] J. Cai and N. Chen, J. Phys.: Condens. Matter **19**, 266207 (2007).

[21] S. Limpijumnong and W. R. L. Lambrecht, Phys. Rev. Lett. **86**, 91 (2001).

[22] A. M. Saitta and F. Decremps, Phys. Rev. B **70**, 035214 (2004).

[23] P. Bolhuis, C. Dellago, and D. Chandler, Faraday Discuss. **110**, 421 (1998).

[24] D. Zahn and S. Leoni, Phys. Rev. Lett. **92**, 250201 (2004).

[25] D. Zahn, O. Hochrein, and S. Leoni, Phys. Rev. B **72**, 094106 (2005).

[26] S. Leoni, Chem.-Eur. J. **13**, 10022 (2007).

[27] S. E. Boulfelfel, D. Zahn, O. Hochrein, Y. Grin, and S. Leoni, Phys. Rev. B **74**, 094106 (2006).

[28] S. E. Boulfelfel, D. Zahn, Y. Grin, and S. Leoni, Phys. Rev. Lett. **99**, 125505 (2007).

[29] H. G. von Schnering and R. Nesper, Z. Phys. B: Condens. Matter **83**, 407 (1991).

[30] H. G. von Schnering and R. Nesper, Angew. Chem. **99**, 1097 (1987); Angew. Chem., Int. Ed. Engl. **26**, 1059 (1987).

[31] Y. Grin, U. Wedig, F. Wagner, H. G. von Schnering, and A. Savin, J. Alloys Compd. **255**, 203 (1997).

[32] S. Leoni and R. Nesper, Acta Crystallogr., Sect. A: Found. Crystallogr. **56**, 383 (2000).

[33] S. Leoni and D. Zahn, Z. Kristallogr. **219**, 339 (2004).

[34] H. G. von Schnering, A. Zürn, J.-H. Chang, M. Baitinger, and Y. Grin, Z. Anorg. Allg. Chem. **633**, 1147 (2007).

[35] S. Leoni (unpublished).

[36] D. J. Binks and R. W. Grimes, J. Am. Ceram. Soc. **76**, 2370 (1993).

[37] A. Chroneos and G. Busker, Acta Chim. Slov. **52**, 417 (2005).

[38] X. W. Sun, Z. J. Liu, Q. F. Chen, H. W. Lu, T. Song, and C. W. Wang, Solid State Commun. **140**, 219 (2006).

[39] G. V. Lewis and C. R. A. Catlow, J. Phys. C **18**, 1149 (1985).

[40] A. Zaoui and W. Sekkal, Phys. Rev. B **66**, 174106 (2002).

[41] Transition pressure $p_c$=13 GPa, bulk modulus $B(B4)$ =133.75 GPa, $B(B1)$=176.15 GPa. The transition pressure is obtained from the intersection of enthalpy ($H$) versus pressure curves, with $H_{B4}$=$H_{B1}$. The parameter $u$ is 0.3815, in good agreement with (Ref. 42).

[42] J. Uddin and G. E. Scuseria, Phys. Rev. B **74**, 245115 (2006).

[43] J. M. Soler, E. Artacho, J. D. Gale, A. García, Javier Junquera, Pablo Ordejón, and Daniel Sánchez-Portal, J. Phys.: Condens. Matter **14**, 2745 (2002).

[44] J. P. Perdew, K. Burke, and M. Ernzerhof, Phys. Rev. Lett. **77**, 3865 (1996).

[45] W. Smith and T. J. Forester, J. Mol. Graphics **14**, 136 (1996).

[46] S. Melchionna, G. Ciccotti and B. L. Holian, Mol. Phys. **78**, 533 (1993).

[47] A. J. Kulkarni, K. Sarasamak, J. Wang, F. J. Ke, S. Limpijumnong, and M. Zhou, Mech. Res. Commun. **35**, 73 (2008).

[48] P. Ruterana, M. Abouzaid, A. Béré, and J. Chen, J. Appl. Phys. **103**, 033501 (2008).